Cross-sectional transmission electron microscopy observations of structural damage in Al 0.16 Ga 0.84 N thin film under contact loading

Sheng-Rui Jian, Jenh-Yih Juang, and Yi-Shao Lai

Citation: Journal of Applied Physics **103**, 033503 (2008); doi: 10.1063/1.2836939
View online: http://dx.doi.org/10.1063/1.2836939
View Table of Contents: http://scitation.aip.org/content/aip/journal/jap/103/3?ver=pdfcov
Published by the AIP Publishing

Cross-sectional transmission electron microscopy observations of structural damage in $Al_{0.16}Ga_{0.84}N$ thin film under contact loading

Sheng-Rui Jian,[1,a)] Jenh-Yih Juang,[2] and Yi-Shao Lai[3]
[1]*Department of Materials Science and Engineering, I-Shou University, Kaohsiung 840, Taiwan*
[2]*Department of Electrophysics, National Chiao Tung University, Hsinchu 300, Taiwan*
[3]*Central Labs, Advanced Semiconductor Engineering, Inc., Kaohsiung 811, Taiwan*

(Received 21 May 2007; accepted 24 November 2007; published online 4 February 2008)

This article reports a nanomechanical response study of the contact-induced deformation behavior in $Al_{0.16}Ga_{0.84}N$ thin film by means of a combination of nanoindentation and the cross-sectional transmission electron microscopy (XTEM) techniques. $Al_{0.16}Ga_{0.84}N$ thin film is deposited by using the metal-organic chemical vapor deposition method. Hardness and Young's modulus of the $Al_{0.16}Ga_{0.84}N$ films were measured by a Berkovich nanoindenter operated with the continuous contact stiffness measurements mode. The obtained values of the hardness and Young's modulus are 19.76 ± 0.15 and 310.63 ± 9.41 GPa, respectively. The XTEM images taken in the vicinity just underneath the indenter tip revealed that the multiple "pop-ins" observed in the load-displacement curve during loading are due primarily to the activities of dislocation nucleation and propagation. The absence of discontinuities in the unloading segments of the load-displacement curve suggests that no pressure-induced phase transition was involved. © *2008 American Institute of Physics*. [DOI: 10.1063/1.2836939]

I. INTRODUCTION

$Al_xGa_{1-x}N$ (AlGaN) thin films are materials with good thermal and chemical stability and, more importantly, with wide direct band gap, which is tunable from 3.4 to 6.2 eV by changing the Al content. Consequently, AlGaN has emerged as one of the most promising materials for numerous optoelectronic applications in the ultraviolet (UV) spectral region.[1,2] For instance, metal-semiconductor-metal UV photodetectors made of $Al_{0.16}Ga_{0.84}N$ have recently been demonstrated to have characteristics of very sharp cutoff wavelength of 330 nm under −10 V bias with more than two orders of magnitude of UV/visible contrast.[3] However, while most of the research has been concentrated on its optoelectronic characteristics, studies on the mechanical characterizations have not drawn equal attention. The mechanical properties of materials are size dependent. Thin films may have different mechanical properties from their bulk materials. Therefore, a precise measurement of the mechanical properties of AlGaN thin films is required in order to use them as structural/functional elements in the devices. The mechanical characteristics and related deformation mechanisms of AlGaN thin films are therefore of significant importance technologically, with contact-induced damage and cracking being of particular interest.

Nanoindentation has proven to be a powerful technique in providing information on mechanical properties (hardness and elastic modulus) of the investigated materials and the variation of these properties with the penetration depth, based on analysis of the respective load-displacement curves[4–9] while also producing contact-induced damage. While diamond anvil cell experiments are capable of investigating the mechanical and phase transformation in bulk materials under hydrostatic pressure,[10] the materials behavior under nanoindentation is of more relevance to realistic contact loading conditions. Particularly, the highly localized nature of the nanoindentation technique makes it ideal for simulating the materials damage introduced during semiconductor nanoprocessing.[11–13]

Nevertheless, the nanoindentation technique itself does not provide the information of subsurface nanoindentation-induced deformation mechanisms and dislocation propagation. The focused ion beam (FIB) miller, which is now widely used for a range of material characterization applications,[14] can be applied to readily image and prepare the cross-sections of materials. FIB can also be used in the preparation of transmission electron microscopy (TEM) lamella, especially for samples that have been locally deformed. Consequently, the subsurface deformation mechanisms operating both within the film and in the vicinity of film/substrate interface following nanoindentation can be directly observed using these FIB-based techniques.

In this study, nanoindentation experiments have been utilized to obtain the mechanical characteristics of $Al_{0.16}Ga_{0.84}N$ films prepared by metal-organic chemical vapor deposition (MOCVD). By combining the load-displacement data with observations of nanoindentation in cross-section, using scanning electron microscopy (SEM) and cross-sectional TEM (XTEM), important aspects of the contact-induced deformation mechanisms of $Al_{0.16}Ga_{0.84}N$ thin film were revealed. The results obtained in this study may also have technological implications for estimating possible mechanical damages induced by the fabrication processes of making the AlGaN-based devices.

[a)]Tel: +886-7-6577711 ext. 3130. Fax: +886-7-6578444. Electronic mail: srjian@gmail.com.

II. EXPERIMENTAL DETAILS

$Al_{0.16}Ga_{0.84}N$ thin films used in this study were grown on (0001)-sapphire substrates by using the MOCVD method with an average thickness of about 1 μm. The details of growth procedures in preparing these AlGaN thin films can be found elsewhere.[5]

The nanoindentation tests are performed on MTS Nano Indenter® XP (MTS Cooperation, Nano Instruments Innovation Center, TN, USA) with a continuous contact stiffness measurement (CSM) technique, which was accomplished by superimposing a small oscillation on the force signal and measuring the displacement response at the same frequency of 75 Hz. A diamond pyramid-shaped Berkovich-type indenter tip (whose radius of curvature is ~50 nm) is employed for the indentation experiments. The nanoindentation tests are carried out in the following sequence: first, the indenter was loaded and unload three times to ensure that the tip was properly in contact with the surface of the materials and that any parasitic phenomenon is released from the measurements. Then, the indenter was loaded for the fourth and final time at a strain rate of 0.05 s^{-1}, with a 60 s hold period inserted at peak load. The analytic method developed by Oliver and Pharr[9] was adopted to determine the hardness (H) and Young's modulus (E) of $Al_{0.16}Ga_{0.84}N$ film from the load-displacement curve. Furthermore, in order to delineate the details of the contact-induced deformation mechanisms, direct microstructure observations, enabled by combining the FIB and TEM techniques, were carried out.

In our measurements, first, a 20×3 indentation array with each indentation being separated by 100 μm to avoid interindent interactions was produced with an indentation load of 200 mN. In each indentation, the Berkovich diamond indenter was operated with the same loading/unloading rate (10 mN/s) and was held at the peak load for 30 s. The XTEM samples were prepared by the lift-out technique using a dual-beam FIB station (FEI Nova 220). The technique for material preparation using the FIB consisted of first milling two crosses alongside the indented area, acting as markers, and then depositing a 1 μm thick layer of Pt to protect the area of interest from Ga^+ ion beam damage and implantation. Material was removed from both sides of the selected area using an ion current of 5 nA, followed by successive thinning steps using decreasing currents from 3 nA to 300 pA until the lamella was about 1 μm thick. Subsequently, the bottom and one side of the lamella were cut free while tilting the specimen at an angle of 45° to the ion beam. A central area containing the indentation apex of a few micrometers in length was then chosen and thinned further to a thickness of 100 nm, leaving at the sides thicker areas that prevented the lamella from collapsing. Finally, a small area of interest was selected and thinned until electron transparency was achieved. The transfer of the lamella from the sample holder to the TEM grid with a carbon membrane was made *ex situ* using the electrostatic force of a glass needle. The XTEM lamella was examined in a JEOL 2010F TEM operating at 200 kV with a point-to-point resolution of 0.23 nm and a lattice resolution of 0.10 nm.

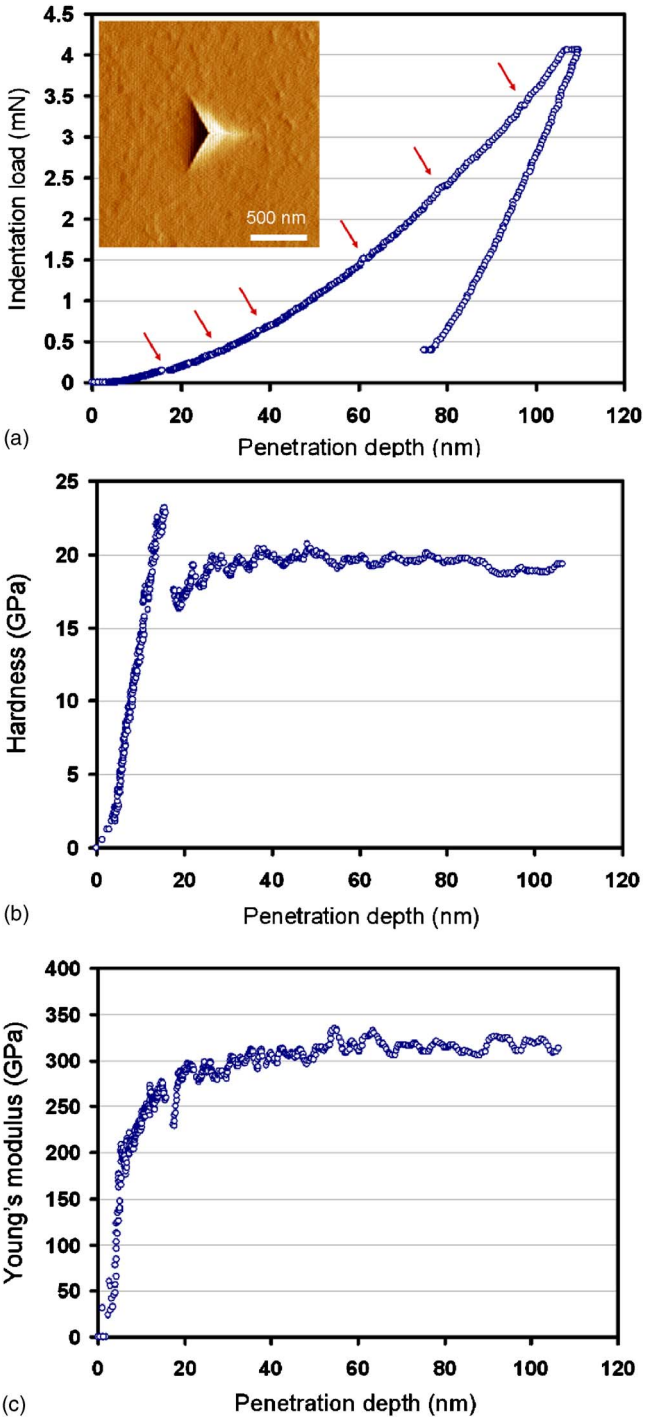

FIG. 1. (Color online) Nanoindentation test results: (a) a load-displacement curve of $Al_{0.16}Ga_{0.84}N$ thin film showing the multiple "pop-ins" (arrows) during loading. Inset: The corresponding AFM nanoindented image. (b) Hardness-displacement curve and (c) Young's modulus-displacement curve for $Al_{0.16}Ga_{0.84}N$ thin film.

III. RESULTS AND DISCUSSION

Figure 1(a) illustrates the typical nanoindentation curve obtained for $Al_{0.16}Ga_{0.84}N$ thin film. The total penetration depth into thin film was ~110 nm with a peak load of 4 mN. The hardness and Young's modulus of $Al_{0.16}Ga_{0.84}N$ thin film can be calculated from the load-displacement data by the analytic method developed by Oliver and Pharr.[9] In addition, with the continuous contact stiffness measurements, the pen-

TABLE I. Mechanical properties of AlGaN thin films obtained in this study and those reported in the literature.

Samples	H (GPa)	E (GPa)	P^* (mN)	τ_{max} (GPa)
$Al_{0.16}Ga_{0.84}N$ [a]	19.76 ± 0.15	310.63 ± 9.41	0.14 ± 0.02	31.01 ± 0.04
$Al_{0.12}Ga_{0.88}N$ [b]	19.24 ± 4.76	315.23 ± 43.09	1.29 ± 0.11	2.98 ± 0.49
$Al_{0.17}Ga_{0.83}N$ [c]	~19.8	371 ± 4	1.35	7.1 ± 0.3
$Al_{0.21}Ga_{0.79}N$ [c]	~19.7	382 ± 5	1.45	7.6 ± 0.6
$Al_{0.27}Ga_{0.73}N$ [c]	~19.5	380 ± 4	0.8	6.3 ± 0.3

[a]Present work.
[b]Reference 5.
[c]Reference 15.

etration depth dependence of the hardness and Young's modulus can be obtained, shown in Figs. 1(b) and 1(c).

It is interesting to note the load-displacement curve in Fig. 1(a), which exhibits irregularities in the course of plastic deformation characterized by the multiple discontinuities at certain penetration depths (see arrows), referred to as "pop-ins." This observation is in contrast to that reported in the previous studies of AlGaN thin films,[5,15] where only a single "pop-in" was observed. The origin of this discrepancy is not clear at present. We speculate that different operating modes may lead to the dissimilar nanoindentation results. Moreover, it is noted that the events of multiple pop-ins are coinciding nicely with sudden decreases in the hardness of measured materials.[16] As can be seen in Fig. 1(b), the hardness of $Al_{0.16}Ga_{0.84}N$ thin film decreases abruptly at the penetration depth of ~18 nm corresponding to the first pop-in event. The hardness after the first pop-in for $Al_{0.16}Ga_{0.84}N$ thin film remains nearly constant at 19.76 ± 0.15 GPa with small fluctuations, possibly associated with dislocation activities. Similarly, as shown in Fig. 1(c), the Young's modulus of $Al_{0.16}Ga_{0.84}N$ films also displays a sudden drop occurring around the same penetration depth and then remains relatively constant at 310.63 ± 9.41 GPa. As is compared in Table I, the Young's modulus obtained in the present study is significantly smaller than those reported by Cáceres *et al.*,[15] albeit similar values for hardness were obtained.

Figure 2 shows the similar load-displacement results obtained with a much larger load of 200 mN and deeper penetration up to 900 nm. Although the resolution was much reduced due to larger indentation load, similar multiple pop-ins are evident. The fact that multiple pop-ins are observable over such a wide range of indentation load and penetration depth indicates the close relations to the plastic deformation of the film. Furthermore, since the multiple pop-ins are randomly distributed on the loading curve in Figs. 1(a) and each curve is associated with a different stress rate, which increases with the maximum indentation load, it is suggestive that the first pop-in is not thermally activated. Instead, these phenomena are usually attributed to dislocation nucleation and propagation during loading, as have been observed in a wide variety of materials,[17,18] or micro-cracking.[19] In addition, the reverse discontinuities during the unloading curve, the so-called "pop-out" event, commonly observed in silicon and attributed to pressure-induced phase transition,[20,21] is not observed here. Thus, it is clear that the first pop-in event may reflect the transition from perfectly elastic to plastic deformation, that is, it is the onset of plasticity in $Al_{0.16}Ga_{0.84}N$ thin film. The corresponding shear stress under the Berkovich indenter at indentation load P^*, where the load-displacement discontinuity occurs, can be determined by using the following relation:[22]

$$\tau_{max} = 0.31\left(\frac{6P^*E^2}{\pi^3R^2}\right)^{0.33}, \quad (1)$$

where R is the radius of the tip of the indenter, and E is defined in terms of Young's moduli and Poisson's ratios of the diamond indenter and thin film. Comparisons of our measurement results of mechanical properties of AlGaN thin films with those reported by previous studies are presented in Table I. Again, the large critical shear stress τ_{max} obtained in this study may arise from the measuring method used.

Returning to the multiple pop-in behaviors displayed by the AlGaN thin films, it should be noted that similar phenomena have been observed previously in hexagonal structured sapphire,[23] GaN thin films,[24] and single-crystal bulk ZnO.[25] On the other hand, materials with cubic structure such as InP and GaAs exhibited only single pop-in characteristic.[26] One possible mechanism being proposed to explain the observed behavior was the slipping systems available for the formation and propagation of dislocations in the material. The multiple slipping systems inherent to hexagonal structure materials are believed to be the primary reason for the resulting multiple pop-ins phenomena. In addition, the SEM observation shown in the inset of Fig. 2 does not reveal any evidence of material pile-ups and signs of crack formation on the film surface around the indented area. Since there are no multiple "pop-outs" on the unloading curves either (Fig. 2), this suggests that phase transitions like that observed in indented Si (Ref. 20) probably are not occurring in the present case. The above discussions indicate that nanoindentation-induced deformation in $Al_{0.16}Ga_{0.84}N$ thin film is predominantly due to dislocation nucleation and propagations. This plastic deformation process is complex and further studies will be necessary to delineate what happens to the material as the indenter penetrates into the surface. The nanoindentation-induced de-

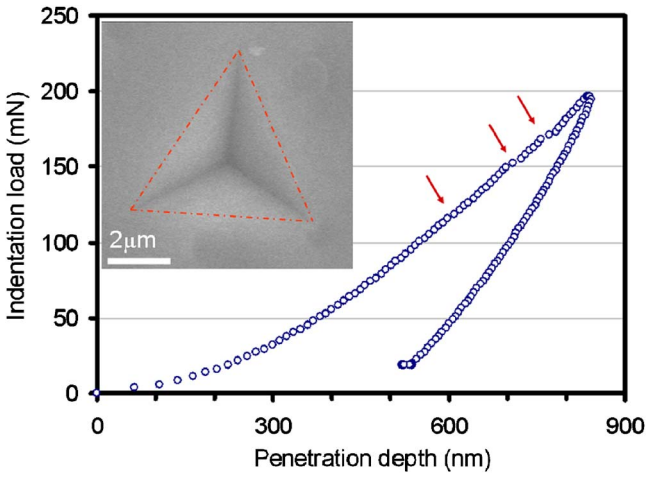

FIG. 2. (Color online) SEM micrograph (inset) of a Berkovich indentation on $Al_{0.16}Ga_{0.84}N$ thin film obtained at an indentation load of 200 mN and the multiple "pop-ins" also displayed in the load-displacement curve.

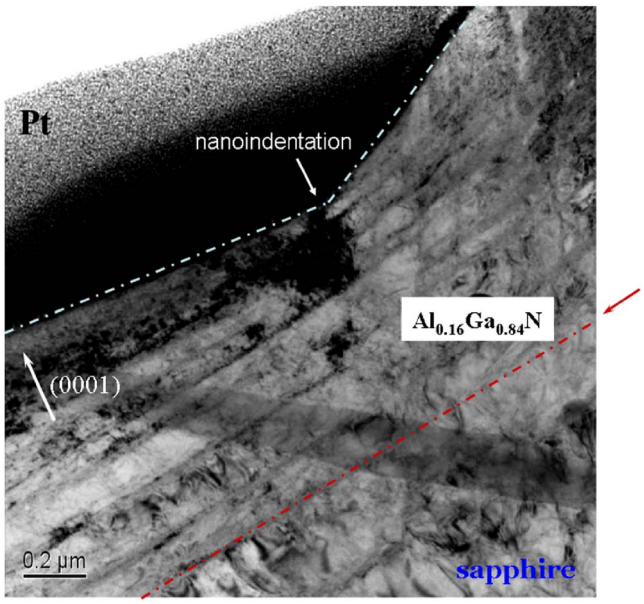

FIG. 3. (Color online) Bright-field XTEM image of $Al_{0.16}Ga_{0.84}N$ thin film subjected to an indentation load of 200 mN.

formation mechanisms will be discussed in more detail with the aid of XTEM techniques in the following.

A bright-field XTEM image of $Al_{0.16}Ga_{0.84}N$ thin film after being indented with an indentation load of 200 mN is displayed in Fig. 3. It clearly displays that, within this thin film, the deformation features underneath the indented spot are primarily manifested by dislocation activities. Namely the slip bands are aligning parallel to the {0001} basal planes all the way down to the thin-film–substrate interface. It is also interesting to note that the heavily strained features in the vicinity of the interface may not be just accidental artifacts resulting from sample preparation. It might be direct evidence for displaying that, because of the excellent interface epitaxy between thin film and substrate, the effects of nanoindentation have, in fact, extended into the sapphire substrate. This argument may also partially explain that, due to the ease of relaxing the local stress right under the indenter's tip via the massive substrate, indentation-induced phase transitions were rarely observed.

In the present study, in addition to those aligning parallel to $Al_{0.16}Ga_{0.84}N$-sapphire interface along the (0001) basal planes, slip bands oriented at ~60° to the sample surface can also be found. The ~60° slip bands, which are believed to originate from dislocations gliding along the $\{10\bar{1}1\}$ pyramidal planes, however, are distributing in much shallower regions near the contacting surface. It is indicative that much higher stress level is needed to activate this slip system as compared to the one along the basal planes. The distorted slip bands and the extremely high dislocation densities at the intersections indicate a highly strained state of the material. Nevertheless, even at the submicron scale, no evidence of subsurface cracking and thin film fragmentation was observed. In addition, the selected area diffraction (not shown here) of the heavily damaged regions did not show evidence of newly formed phases either.

In closing, from the above observations and discussion, it is apparent that, in the Berkovich indentation scheme, the primary deformation mechanism for $Al_{0.16}Ga_{0.84}N$ thin film is dislocation nucleation and propagation along easy slip systems. Since the multiple pop-ins are usually observed after permanent plastic deformation has occurred and two of the possible mechanisms, the deformation-induced phase transition[20,27] and fracture of thin films,[19] were basically ruled out, the most likely mechanism responsible for the multiple pop-ins appears to be associated with the activation of dislocation sources.[28] In this scenario, plastic deformation prior to the pop-in event is associated with the individual movement of a small number of newly nucleated and preexisting dislocations. As the number of dislocations is increased and entangled to each other, large shear stress is quickly accumulated underneath the indenter tip. When the local stress underneath the tip reaches some threshold level, a burst of collective dislocation movement on the easy slip systems is activated, leading to a large release of local stress and a pop-in event on the load-displacement curve. Each of these collective dislocation movements is reflected as a slip band in the indented microstructure displayed in Fig. 3. Notice that, although the slip bands appeared to stop near the thin-film–substrate interface, the released stress due to this effect could extend deep into the substrate as mentioned above. Moreover, the narrow spacing of the dense bands of defects and/or dislocations along the basal planes near the surface suggests that, in the later stage of indentation, a large indentation load, such as the 200 mN used in the present experiments, starts to activate extensive slip bands along the ~60° pyramidal planes. The extensive interactions between the dislocations slipping along the two slip systems, therefore, confined the slip bands in a shallow regime, which, in turn, resulted in a heavily deformed and strain-hardened lattice structure. Finally, we note that the so-called "slip-stick" behavior,[29] characterized by material pile-ups caused by interactions between the as-grown defects and the nanoindentation-induced dislocations, is not significant in this study. Whether it is due to the insignificant grown-in defect density of our AlGaN films or is related to the specific geometric shape of the indenter tip used is not clear at present and further studies may be required to clarify this issue.

IV. CONCLUSION

To summarize, in this study the mechanical responses of MOCVD $Al_{0.16}Ga_{0.84}N$ thin film to nanoindentation have been investigated by combining nanoindentation and microscopic techniques. Multiple "pop-ins" were observed in the load-displacement curves and appeared to occur randomly with increasing indentation load. These instabilities are attributed to the dislocation nucleation and propagation. No evidence of either phase transformation or formation of micro-cracking was observed by AFM, SEM, and even XTEM. The absence of nanoindentation-induced new phases might have been due to the stress relaxation via substrate and is also consistent with the fact that no discontinuity was found upon unloading. Moreover, it is noted that both the basal and pyramidal planes of $Al_{0.16}Ga_{0.84}N$ lattice are acting

as the primary slip systems for collective dislocation motions, with the latter being activated at a higher stress state and hence a later stage of indentation. The hardness and Young's modulus of $Al_{0.16}Ga_{0.84}N$ thin film estimated using the continuous stiffness operation mode provided with the nanoindenter are 19.76 ± 0.15 and 310.63 ± 9.41 GPa, respectively.

ACKNOWLEDGMENTS

This work was partially supported by National Science Council of Taiwan through Grant No. NSC 96-2112-M-214-001.

[1]T. D. Moustakas, E. Iliopoulos, A. V. Sampath, H. M. Ng, D. Doppalapudi, M. Misra, D. Korakakis, and R. Singh, J. Cryst. Growth **227–228**, 13 (2001).
[2]M. Asif Khan, M. Shatalov, H. P. Maruska, H. M. Wang, and E. Kuokstis, Jpn. J. Appl. Phys., Part 1 **44**, 7191 (2005).
[3]D. W. Kim, K. S. Chea, Y. J. Park, I. H. Lee, and C. R. Lee, Phys. Status Solidi A **201**, 2686 (2004).
[4]X. D. Li, H. Gao, C. J. Murphy, and K. K. Caswell, Nano Lett. **3**, 1495 (2003).
[5]S.-R. Jian, T.-H. Fang, and D.-S. Chuu, J. Electron. Mater. **32**, 496 (2003).
[6]X. D. Li, H. Gao, C. J. Murphy, and L. Gou, Nano Lett. **4**, 1903 (2004).
[7]X. D. Li, X. Wang, Q. Xiong, and P. C. Eklund, Nano Lett. **5**, 1982 (2005).
[8]S.-R. Jian, T.-H. Fang, and D.-S. Chuu, Appl. Surf. Sci. **252**, 3033 (2006).
[9]W. C. Oliver and G. M. Pharr, J. Mater. Res. **7**, 1564 (1992).
[10]A. Mujica, A. Rubio, A. Muñoz, and R. J. Needs, Rev. Mod. Phys. **75**, 863 (2003).
[11]J. H. A. Hagelaar, E. Bitzek, C. F. J. Flipse, and P. Gumbsch, Phys. Rev. B **73**, 045425 (2006).
[12]Q. Tang and F. Chen, J. Phys. D **39**, 3674 (2006).
[13]S.-R. Jian, T.-H. Fang, D.-S. Chuu, and L.-W. Ji, Appl. Surf. Sci. **253**, 833 (2006).
[14]K. Wasmer, C. Ballif, R. Gassilloud, C. Pouvreau, R. Rabe, J. Michler, J. M. Breguet, J. M. Solletti, A. Karimi, and D. Schulz, Adv. Eng. Mater. **7**, 309 (2005).
[15]D. Cáceres, I. Vergara, R. González, E. Monroy, F. Calle, E. Muñoz, and F. Omnès, J. Appl. Phys. **86**, 6773 (1999).
[16]J. E. Bradby, J. S. Williams, and M. V. Swain, J. Mater. Res. **19**, 380 (2004).
[17]D. F. Bahr, D. E. Kramer, and W. W. Gerberich, Acta Mater. **46**, 3605 (1998).
[18]A. J. Haq, P. R. Munroe, M. Hoffman, P. J. Martin, and A. Bendavid, Thin Solid Films **515**, 1000 (2006).
[19]S. J. Bull, J. Phys. D **38**, R393 (2005).
[20]J. E. Bradby, J. S. Williams, J. Wong-Leung, M. V. Swain, and P. Munroe, Appl. Phys. Lett. **77**, 3749 (2000).
[21]J. E. Bradby, J. S. Williams, J. Wong-Leung, M. V. Swain, and P. Munroe, J. Mater. Res. **16**, 1500 (2001).
[22]K. L. Johnson, *Contact Mechanics* (Cambridge U. P., Cambridge, UK, 1985).
[23]R. Nowak, T. Sekino, S. Maruno, and K. Niihara, Appl. Phys. Lett. **68**, 1063 (1996).
[24]S. O. Kucheyev, J. E. Bradby, J. S. Williams, C. Jagadish, M. V. Swain, and G. Li, Appl. Phys. Lett. **78**, 156 (2001).
[25]S. O. Kucheyev, J. E. Bradby, J. S. Williams, C. Jagadish, and M. V. Swain, Appl. Phys. Lett. **80**, 956 (2002).
[26]J. E. Bradby, J. S. Williams, J. Wong-Leung, M. V. Swain, and P. Munroe, Appl. Phys. Lett. **78**, 3235 (2001).
[27]D. J. Oliver, J. E. Bradby, J. S. Williams, M. V. Swain, and P. Munroe, J. Appl. Phys. **101**, 043524 (2007).
[28]Y. Gaillard, C. Tromas, and J. Woirgard, Philos. Mag. Lett. **83**, 553 (2003).
[29]J. E. Bradby, S. O. Kucheyev, J. S. Williams, J. Wong-Leung, M. V. Swain, P. Munroe, G. Li, and M. R. Phillips, Appl. Phys. Lett. **80**, 383 (2002).